

Insights into the Effect of Hydrate Dissociation, induced by Climate Change, on the Stability of an Arctic Continental Slope

K. P. Lijith*¹, and Jeffrey A. Priest¹

¹*Department of Civil Engineering, University of Calgary, Calgary, Canada*

**Corresponding author's email: lijith.koorthedathpu@ucalgary.ca*

Abstract: Hydrate dissociation resulting from Arctic warming has been inferred from observations of seafloor seepage of gas on the continental slope of the Arctic Ocean. Dissociation of gas hydrate within clay-rich marine sediments, which are typically found on the Arctic Ocean margins, can dramatically weaken the strength of the host sediment and may lead to submarine slope failures. To consider the impact of global warming on slope stability in the Arctic, two-dimensional numerical simulations were conducted using sequential thermal-hydrologic-mechanical coupling between TOUGH+HYDRATE and FLAC3D. The simulations considered the spatiotemporal variations in the hydrate saturation in the hydrate-bearing strata and the evolution in pore-pressure, shear strength and stiffness during a warming event. The hydrate dissociation kinetics, fluid flow and heat migration within the hydrate-bearing sediments on the Arctic continental slope were modelled using TOUGH+HYDRATE, while the geomechanical response of the system is captured using FLAC3D. The study considered various factors associated with the warming of the Arctic Ocean over 150 years timeline, including ocean warming rate, seafloor slope gradient, and hydrate saturation. The results suggest that instabilities or slips would occur at the small scale, while large-scale submarine landslides are unlikely to result from hydrate dissociation within the time span considered in the study.

Introduction

Natural gas hydrates, referred to as gas hydrates hereafter, are distributed worldwide within deep-water marine sediments and below permafrost and contribute to the global carbon cycle by storing large volumes of methane gas. Gas hydrates are metastable clathrates of methane trapped in water cages and their stability predominantly depends on the combination of pressure and temperature, which is referred to as the hydrate stability zone. Rises in ocean temperatures or change in sea levels can alter the pressure or temperature of gas hydrates to an extent that the gas hydrates dissociate, releasing methane gas and water. Gas hydrates on the Arctic continental slope are more sensitive to changes in global climate due to their formation at shallower depths that results from the relatively lower ocean temperatures at a given water depth in this region [1-2]. Methane gas seeps along the Arctic continental slope that coincides with the feathered edge of the hydrate stability region have been inferred to result from increase

in temperature resulting from climate change in the region [3]. In addition, seafloor structures associated with the dissociation of hydrates, such as pockmarks and craters are routinely observed on the western Svalbard margin and the Barents Sea in the Arctic region.

Numerous studies have sought to consider the impact of hydrate dissociation on the stability of continental slopes, resulting from ocean warming or changes in sea-level. Nixon and Grozic [6] investigated the increase in pore-pressure due to the release of methane gas during hydrate dissociation, highlighting its adversely affect on slope stability. A two-dimensional limit equilibrium slope stability analysis conducted by Priest and Grozic [1] reported the likelihood of slope instabilities, such as surficial sloughing to deep-seated failures resulting from Arctic warming-induced hydrate dissociation. However, these studies did not consider factors such as hydrate dissociation kinetics, geomechanics, fluid flow, and heat transport, which were deemed to be imperative to capture the complexities associated with modeling hydrate dissociation in marine sediments. Rutqvist and Moridis [7] put forth a workflow to model the thermal-hydrological-mechanical processes associated with gas hydrate-bearing sediments by sequentially coupling the software, TOUGH+HYDRATE [8] and FLAC3D [9]. Dhakal and Gupta [10] and Liu *et al.* [11] employed this approach to assess the deformations in slopes of the Northern Cascadia Margin and Northern South China Sea resulting from ocean warming and glacial sea-level drop, respectively.

Typically, in the models above, it is assumed that soil strength is enhanced by the presence of hydrate, that it increases linearly with hydrate saturation, and upon dissociation the soil strength reduces in the same linear manner with hydrate saturation back to the strength of the soil without hydrate. However, this behavior was developed based on studies conducted on hydrate-bearing sands [7], where the hydrate is disseminated throughout the pore space in the sand. In fine-grained gas hydrate-bearing marine sediments, the hydrate typically forms sub-vertical veins and fractures that can lead to an apparent increase in shear strength and stiffness of the gas hydrate-bearing sediment. However, the hydrate in this case can impede normal consolidation of the soil, such that the host soil matrix becomes under-consolidated. Gas hydrate-bearing sediment samples recovered from the Krishna-Godavari Basin [19] showed that the soil matrix, after hydrate had been dissociated, gave undrained shear strength as low as ~ 6 kPa, significantly lower than that associated with normally consolidated sediments at the same burial depth [5]. In subsequent laboratory tests, Ma [4] showed that dissociation of the hydrate veins can lead to large deformation of the fine-grained sediments. As such, in fine-grained sediments hydrate dissociation may lead to significant loss of strength of the sediment that has not been fully considered within slope stability simulation.

Given that the Arctic region is undergoing intense climatic changes that may result in the dissociation of shallow hydrates, it is necessary to investigate the interplay between temperature rise, hydrate dissociation and associated deformations of the slope especially when fine-grained gas hydrate-bearing sediments might be encountered. Hence, the present study delves into ocean warming-induced gas hydrate dissociation and the associated deformations

of the continental slope in the Arctic region. It is believed that the understanding developed through this study will be crucial to assess and mitigate the risks gas hydrates poses as a geological hazard.

Methodology

The present study investigates the influence of hydrate dissociation, induced by warming of the Arctic Ocean over the next 150 years, on the stability of a typical Arctic continental slope. To achieve the mentioned objective, two independent numerical simulators are sequentially coupled, named TOUGH+HYDRATE and FLAC3D to model the behavior of the slope during dissociation including coupled fluid flow and heat flow. TOUGH+HYDRATE is a numerical simulator that works based on the mass and energy balance equations, while FLAC3D works based on the principle of momentum balance. For each time step of the sequential coupling, changes in pore-pressure, temperature and phase saturations (viz., hydrate saturation, gas saturation, water saturation) are obtained from TOUGH+HYDRATE, due to change in boundary temperature, which are then imported into the geomechanical FLAC3D simulator to compute the associated deformation using a Mohr-Coulomb elastoplastic mechanic model. The induced strains modelled in FLAC3D are then used to update the porosity and permeability of the sediment and imported back into TOUGH+HYDRATE for the next time step. The data exchange for the sequential coupling is enabled using python code. This sequential modelling is continued until the simulation period ends (150 years). To minimise numerical errors, a short time step of 10 days was employed in the present study. In addition, equivalent grids for TOUGH+HYDRATE and FLAC3D models, with a length and width of 5m were created for exchanging information from each software, using the python library toughio [12].

Following the observations made by the Intergovernmental Panel on Climate Change [13], the sea floor temperature in our model was increased at a rate of $0.03^{\circ}\text{C}/\text{year}$ for 100 years in the present study. After 100 years simulation period, the seafloor temperature was maintained constant for the remaining 50 years. The seafloor layer was assigned an open hydrological boundary condition. The bottom boundary of the model was set to have constant heat flux, which corresponded to a $0.60^{\circ}\text{C}/\text{m}$ geothermal gradient, along with a zero displacement in x and z direction. For the lateral boundaries, zero fluid flow and zero heat flux were assigned along with zero deformations perpendicular to the z direction.

Slope Model Profile and Soil Parameters

A typical submarine slope was considered with a horizontal downslope (x-direction) of 3500m modelled (Figure 1). A seafloor depth (left hand side) of 290m from the sea surface was modelled to correspond to approximate depth of the featheredge of the hydrate stability zone in the Arctic margin. The model depth below seafloor was set at 200m to ensure that this fixed boundary had no influence on simulation response. The model depth and width gave a slope gradient of 3.5° .

The base of the hydrate stability zone was determined using the hydrate stability criterion given by Moridis [14] for 0°C seafloor temperature, 3.5 wt% pore water salinity and 0.60°C/m geothermal gradient. A 5 m thick non-hydrate soil layer was considered directly below the seafloor to account for the sulfate reduction zone [3]. For the hydrate stability zone, a uniform hydrate saturation (S_H) of 20% was assigned based on Rees *et al.* [15], who had conducted micro-CT scanning experiments on hydrate-bearing sediment samples retrieved from the Krishna-Godavari Basin and observed vertical or sub-vertical hydrate veins with S_H ranging between 20-30%.

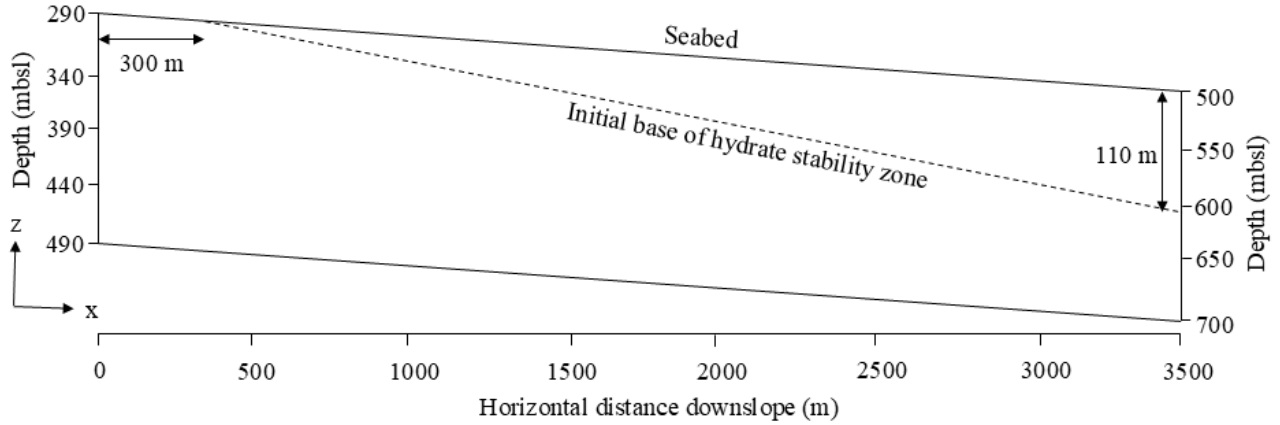


Figure 1: Modelled slope geometry highlighting the ocean bed and initial base of hydrate stability zone.

As mentioned, the Mohr-Coulomb elastoplastic mechanical model was used to model both hydrate-bearing and hydrate-free sediments. However, limited data are available in the literature on the geomechanical properties of gas hydrate-bearing clays. In the present study, the shear strength and stiffness of the hydrate-bearing sediments were considered to decrease exponentially with the reduction in S_H (refer to Table 1) during dissociation. Sultaniya *et al.* [16] reported that thermal stimulation-induced hydrate dissociation results in a rapid decrease in stiffness of the hydrate-bearing sands due to the loss in cementation. Hence, exponential relationships were used in the present study to capture this phenomenon. Furthermore, based on Priest *et al.* [5], a low value of 6 kPa was assigned to cohesion of the completely dissociated hydrate-bearing sediments. For the hydrate-free sediments, the strength and stiffness of the soil were expressed as functions of the vertical effective stress (σ_v') (refer to Table 1). The strength and stiffness considerations employed in the present study track the rapid reduction in strength and stiffness of sediments during dissociation and the gain in their values during post-hydrate dissociation consolidation. The porosity (ϕ) of all sediments was assumed to vary according to mean effective stress (σ_m') and S_H given by,

$$\phi = \phi_r + 0.066 \exp\left(-\frac{\sigma_m' \{in \text{ kPa}\}}{500 + 200 * S_H}\right) \quad (1)$$

$$\phi_r = 0.40 + (0.44 * S_H) \quad (2)$$

where, ϕ_r is residual porosity. A uniform initial value of 10^{-15} m² was assigned for permeability to all soils. The permeability (k) is correlated to the porosity according to following exponential function [18];

$$k = k_0 \exp\left(22.2 * \left\{\frac{\phi}{\phi_0} - 1\right\}\right) \quad (3)$$

where, k_0 and ϕ_0 are the permeability and porosity at zero stress.

Table 1: Material properties for hydrate-bearing and hydrate-free sediments.

Soil layer	Cohesion (kPa)	Young's modulus (MPa)
Hydrate-bearing sediments	$6 \exp(14 * S_H)$	$3 \exp(15 * S_H)$
Hydrate-free sediments	$0.20 \sigma_v'$	$0.8 (\sigma_v')^{0.5}$

The unit of σ_v' is kPa.

Results and Discussion

For the rate of temperature increase considered in the present study, 0.03°C/years, the observed evolution of hydrate saturation (S_H) and gas saturation (S_G) over time is highlighted in Figure 2. After 150 years, hydrate dissociation extended up to 1800m and 1300m on the upper and lower boundaries of the initial gas hydrate stability zone, respectively. The maximum value of S_G was approximately 23%. Simulation results suggest that hydrate dissociation begins around 7 years at the upper left edge of the hydrate stability zone.

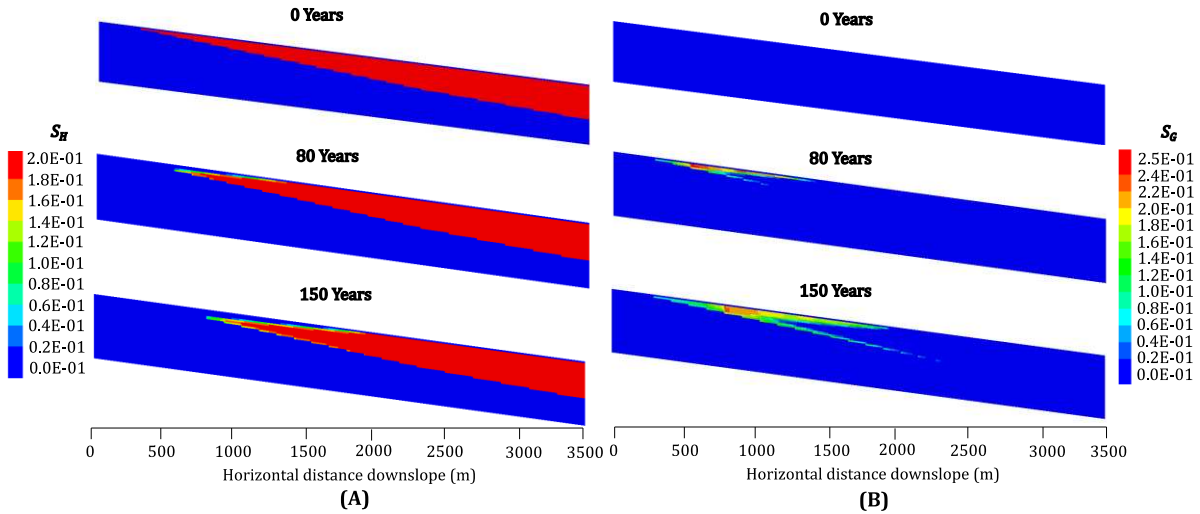


Figure 2: Hydrate saturation (S_H) and gas saturation (S_G) within the system at times 0, 80, and 150 years.

As shown in Figure 2, although hydrate dissociation initiates from both the top and bottom of the hydrate stability zone, the dissociation front expands more rapidly on the top surface of the

hydrate-bearing sediment due to the higher sensitivity of shallow sediments to warming compared to deeper soils. To better illustrate this mechanism, variations in the temperature, S_H and S_G , along a vertical profile at 1000m from the left boundary of the model are presented for different time intervals in Figure 3. It can be observed that hydrate dissociation has not commenced in this section after 40 years of simulated time. However, after 60 years, S_H begins to decrease while S_G increases progressively, continuing up to 150 years. The closely clustered temperature profiles in the hydrate layers indicate that the heat energy from seabed warming is primarily utilised for hydrate dissociation rather than for warming the surrounding strata.

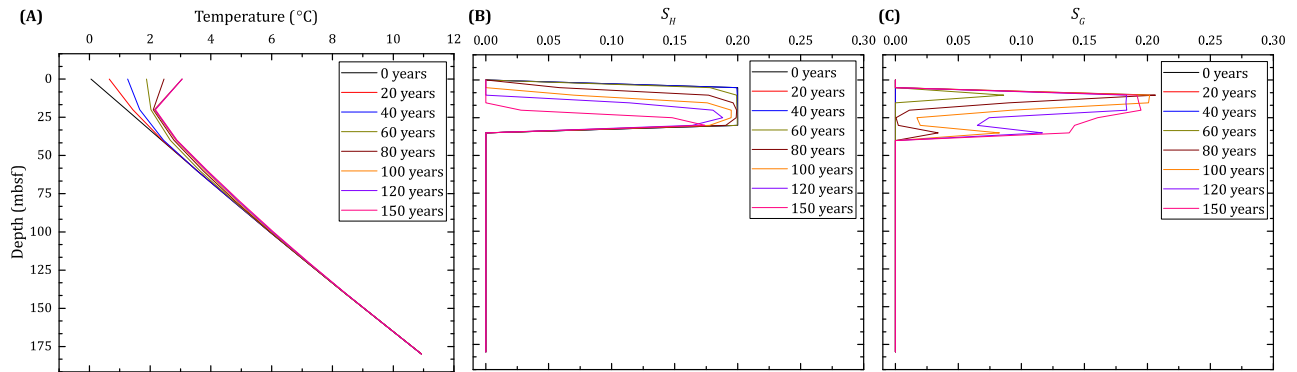


Figure 3: Variation of (A) temperature, (B) hydrate saturation (S_H) and (C) gas saturation (S_G) along the vertical plane at 1000m from the left side of the slope.

It is also seen that as times passes, hydrate dissociation progresses releasing water and methane gas resulting in the development excess pore-pressure. In the case of warming-induced hydrate dissociation, the excess pore-pressure generated depends on the rate of temperature rise (or rate of hydrate dissociation) and drainage conditions [6]. For the conditions considered in the present study, the excess pore-pressure generated due to hydrate dissociation at 100 and 150 years are depicted in Figure 4. The maximum value of the excess pore-pressure was observed to be 30 kPa. It can be noticed from Figure 4 that the excess pore-pressure zone expands with time and progresses downhill surrounding the hydrate dissociation front. After the completion of hydrate dissociation, the excess pore-pressure generated dissipates with time. During this stage, the sediment undergoes consolidation and gains strength and stiffness according to the equations referred in Table 1.

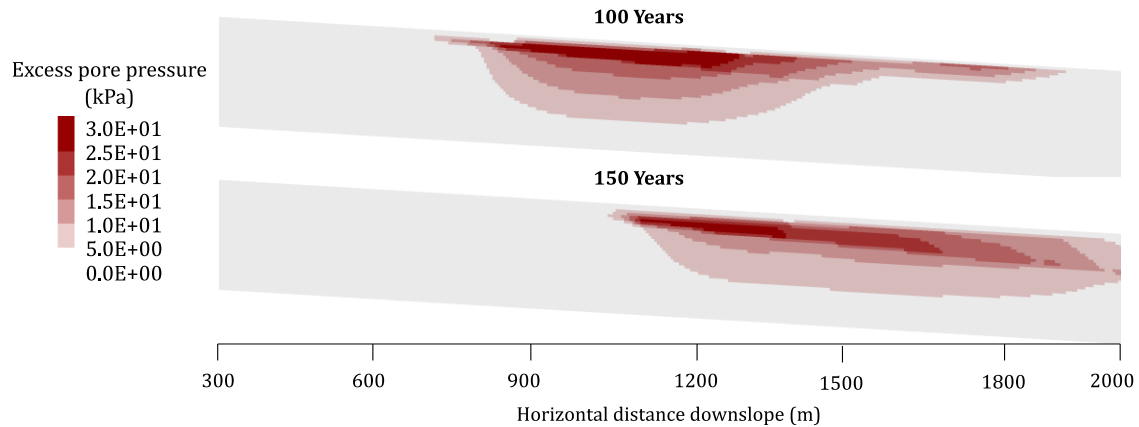


Figure 4: Excess pore-pressure generated in the slope due to the dissociation of hydrates for times 100 and 150 years.

Warming-induced deformations of the slope

The displacement vectors corresponding to 100 and 150 years of warming are depicted in Figure 5. The maximum values for the displacement in the slope were observed to be 0.46 m and 3.70 m for 100 and 150 years, respectively. The simulation results also suggest that as time passes, the magnitude of the displacement increases, with displacements broadly distinguished into compressional and extensional displacements. Generally, compressional displacements were observed on the upper side of the hydrate dissociation front (or in the completely dissociated sediments), while extensional displacements were observed when hydrate dissociation was occurring, and for the lower side of the hydrate dissociation front. During hydrate dissociation, the strength and stiffness of the sediments decrease quickly, and pore-pressure builds up resulting in the extensional displacement (upwards and rightward movement) of the sediments. However, once hydrate dissociation is complete, the excess pore-pressure dissipates, and the sediment undergoes consolidation resulting in compressional displacements. These observations, from the modeling, follow observations made by Mountjoy *et al.* [17], who using seismic reflection and bathymetric surveys on the upper slope of the northern Hikurangi Margin, New Zealand, reported extensional and compressional deformations assumed to correspond to hydrate dissociation.

Figure 6 illustrates the displacements within the slope in the horizontal (x-direction) and vertical (z-direction) directions after 150 years. At this time the maximum extensional displacements (+ve values) in the x-direction (rightward) and z-direction (upward) were observed to be 3.8 m and 0.37 m, respectively. While the compressional displacements (-ve values) for x-direction and z-direction were observed to be 0.1 m and 0.65 m, respectively. The simulation results suggest that for the given conditions (*viz.*, permeability of 10^{-15} m^2 , 3.5° slope gradient and $0.03^\circ\text{C}/\text{year}$ rise in temperature), significant deformations only occur near the seafloor within the sediment column. These results indicate that plastic deformations or mechanical instabilities are limited to the hydrate stability zone at shallow depths. This may

arise due to the presence of gas hydrate-bearing sediments (not undergoing dissociation) downhill of the dissociated front resisting the downslope movement of the weaker sediments that had undergone hydrate dissociation. For a large landslide to occur, a continuous slip surface exhibiting large strains is required, which is not observed. As such, the modelled ground warming conducted in this study is unlikely to lead to large-scale landslide, although local shallow instabilities are prone to occur, which may be of concern for surface infrastructure if located in such regions.

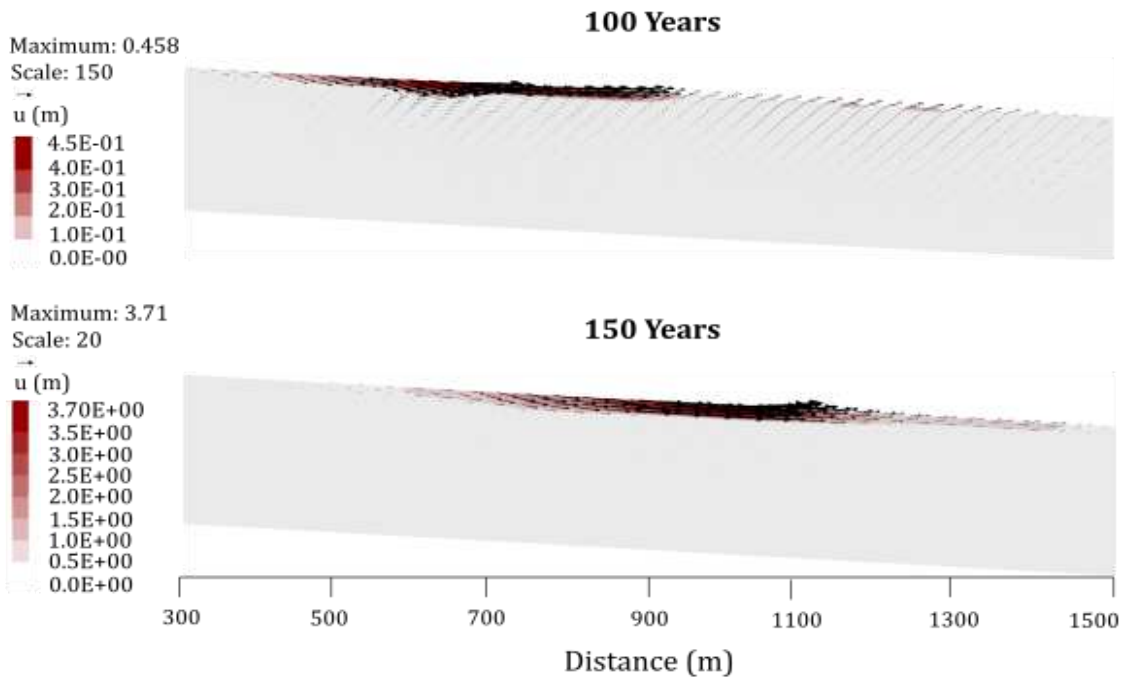


Figure 5: The displacement vectors u (m) for 100 and 150 years.

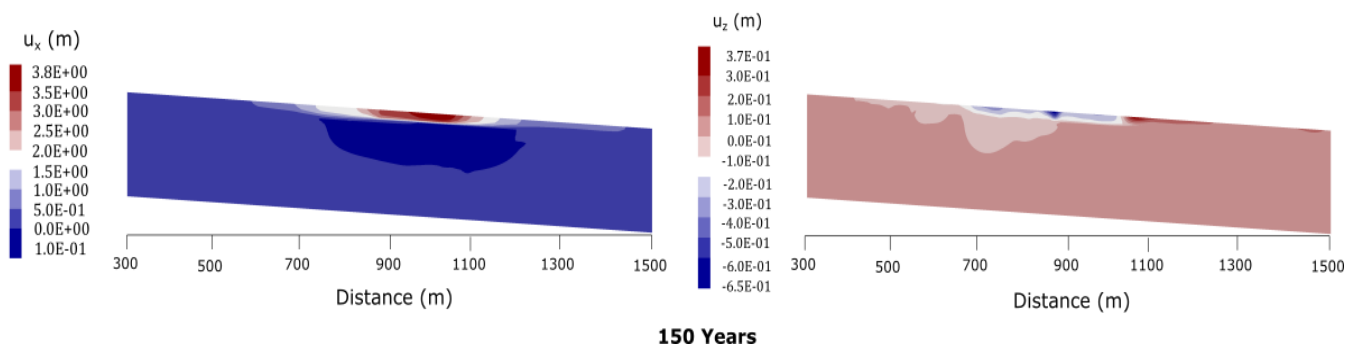


Figure 6: Modelled displacements for 150 years. A positive x-direction displacement (u_x) indicates rightward movement, and a positive z-direction displacement (u_z) indicates upward displacement.

Conclusions

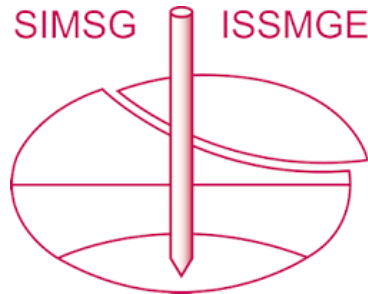
The present study presents a sequential thermal-hydrological-mechanical coupling workflow to assess the impact of climate change-induced hydrate dissociation on the stability of slopes in the Arctic continental margin. The spatiotemporal variations in the shear strength and stiffness of the hydrate-bearing sediments, and evolutions in the excess pore-pressure were modelled to determine the deformations within the slope. Simulation results indicate that the warming of the Arctic Ocean may lead to hydrate dissociation extending up to 1800m downslope. The ensuing dissociation, which leads to a reduction in shear strength and stiffness of the sediments and an increase in pore-pressure, result in compressional and extensional displacements within the slope; however, these displacements were confined to shallow sub-seafloor depths. As such, the likelihood of large-scale landslides was found to be minimal given the slope geometry, soil parameters, and ocean warming temperature gradient considered in this study.

References

- [1] J. A. Priest and J. L. H. Grozic. Stability of fine-grained sediments subject to gas hydrate dissociation in the arctic continental margin. *Adv. Nat. Technol. Hazards Res.*, 41: 427–436, 2016.
- [2] G. K. Westbrook *et al.* Escape of methane gas from the seabed along the West Spitsbergen continental margin. *Geophys. Res. Lett.*, 36(15), 2009.
- [3] A. Biastoch *et al.* Rising Arctic Ocean temperatures cause gas hydrate destabilization and ocean acidification. *Geophys. Res. Lett.*, 38(8), 2011.
- [4] B. Ma. The impact of THF hydrate veins on the consolidation behavior of fine-grained soils. University of Calgary, Calgary, 2020.
- [5] J. A. Priest, C. R. I. Clayton and E. V. L. Rees. Potential impact of gas hydrate and its dissociation on the strength of host sediment in the Krishna–Godavari Basin. *Mar. Pet. Geol.*, 58:187–198, 2014.
- [6] M. F. Nixon and J. L. Grozic. Submarine slope failure due to gas hydrate dissociation: a preliminary quantification. *Can. Geotech. J.*, 44(3), 2007.
- [7] J. Rutqvist and G. J. Moridis. Numerical Studies on the Geomechanical Stability of Hydrate-Bearing Sediments. *SPE J.*, 14: 267–282, 2009.
- [8] G. J. Moridis. User’s manual for the hydrate v1.5 option of TOUGH+v1.5: A code for the simulation of system behavior in hydrate-bearing geologic media. Lawrence Berkeley National Laboratory (LBNL): Berkeley, CA, No. LBNL-6869E, 2014.
- [9] Itasca. FLAC3D Manual: Fast Lagrangian Analysis of Continua in 3 Dimensions Version 6.0. Itasca Consulting Group Inc., 2012.
- [10] S. Dhakal and I. Gupta. Slope instability of submarine sediments due to hydrate dissociation: A case study of Northern Cascadia Margin. *Geoenergy Sci. Eng.*, 223: 211558, 2023.
- [11] J. Liu *et al.* Can Glacial Sea-Level Drop-Induced Gas Hydrate Dissociation Cause Submarine Landslides? *Geophys. Res. Lett.*, 51(6), 2024.
- [12] K. Luu. toughio: Pre- and post-processing Python library for TOUGH. *J. Open Source Softw.*, 5(51), 2020.

- [13] Intergovernmental Panel on Climate Change (IPCC) (2007) Climate change 2007: The Physical Science Basis. Cambridge University Press, New York.
- [14] G. J. Moridis. Numerical studies of gas production from methane hydrates. *Spe J.*, 8(4), 2003.
- [15] E. V. Rees, J. A. Priest and C. R. Clayton. The structure of methane gas hydrate bearing sediments from the Krishna–Godavari Basin as seen from Micro-CT scanning. *Mar. Pet. Geol.*, 28(7), 2011.
- [16] A. Sultaniya, J. A. Priest and C. Clayton. Impact of formation and dissociation conditions on stiffness of a hydrate-bearing sand. *Can. Geotech. J.*, 55(7), 2018.
- [17] J. J. Mountjoy, I. Pecher, S. Henrys, G. Crutchley, P. M. Barnes. and A. Plaza-Faverola. Shallow methane hydrate system controls ongoing, downslope sediment transport in a low-velocity active submarine landslide complex, Hikurangi Margin, New Zealand. *Geochem. Geophys. Geosystems*, 15(11):4137–4156, 2014.
- [18] J. Rutqvist and C. -F. Tsang. A study of caprock hydromechanical changes associated with CO₂ injection into a brine aquifer. *Environmental Geology*, 42(11): 296–305, 2002.
- [19] T. S. Collett et al. National Gas Hydrate Program Expedition 01 initial report. *Dir. Gen. of Hydrocarbons, Minist. of Pet. and Nat. Gas*, New Delhi, 2008.

INTERNATIONAL SOCIETY FOR SOIL MECHANICS AND GEOTECHNICAL ENGINEERING



This paper was downloaded from the Online Library of the International Society for Soil Mechanics and Geotechnical Engineering (ISSMGE). The library is available here:

<https://www.issmge.org/publications/online-library>

This is an open-access database that archives thousands of papers published under the Auspices of the ISSMGE and maintained by the Innovation and Development Committee of ISSMGE.

The paper was published in the proceedings of the 4th Pan-American Conference on Unsaturated Soils (PanAm UNSAT 2025) and was edited by Mehdi Pouragha, Sai Vanapalli and Paul Simms. The conference was held from June 22nd to June 25th 2025 in Ottawa, Canada.